The Relevance of the Microphysical and Radiative Properties of Cirrus Clouds to Climate and Climatic Feedback

GRAEME L. STEPHENS, SI-CHEE TSAY, PAUL W. STACKHOUSE, JR. AND PIOTR J. FLATAU

Department of Atmospheric Science, Colorado State University, Fort Collins, Colorado

(Manuscript received 24 February 1989, in final form 5 February 1990)

ABSTRACT

This paper examines the effects of the relationship between cirrus cloud ice water content and cloud temperature on climate change. A simple mechanistic climate model is used to study the feedback between ice water content and temperature. The central question studied in this paper concerns the extent to which both the radiative and microphysical properties of cirrus cloud influence such a feedback. To address this question, a parameterization of the albedo and emissivity of clouds is introduced. Observations that relate the ice water content to cloud temperature are incorporated in the parameterization to introduce a temperature dependence to both albedo and emittance. The cloud properties relevant to the cloud feedback are expressed as functions of particles size r_e, asymmetry parameter g and cloud temperature and analyses of aircraft measurements, lidar and ground based radiometer data are used to select r_e and g. It was shown that scattering calculations assuming spherical particles with a distribution described by $r_e = 16$ μm reasonably matched the lidar and radiometer data. However, comparison of cloud radiation properties measured from aircraft to those parameterized in this study required values of g significantly smaller than those derived for spheres but consistent with our understanding of non-spherical particle scattering.

The climate simulations revealed that the influence of cirrus cloud on climate was strongly affected by the choice of r_e and g: parameters that are both poorly known for cirrus. It was further shown that the effect of ice water feedback on a CO_2 warming simulation could be either positive or negative depending on the value of r_e assumed. Based on these results, it was concluded that prediction of cirrus cloud feedback on climate is both premature and limited by our lack of understanding of the relationship between size and shape of ice crystals and the gross radiative properties of cirrus.

1. Introduction

Global warming is a contemporary topic of great scientific interest. With the projected rise in sea level and the anticipated effects of climate change on agriculture among others, global warming has escalated to the level of a major societal issue. At the grass-roots scientific level however, global warming has not yet been proclaimed as an accepted truth and it has been realized for some time that potential feedbacks via the effect of cloud on the Earth's radiation budget make nonsense of any prediction of a global temperature rise (Paltridge 1980). A number of recent scientific studies have attempted to investigate the perplexing effects of cloud feedback on global warming. Some of these studies consider that the observed relationships between cloud water content and cloud temperature and the dependence of cloud albedo and cloud emittance on cloud liquid water serves as a mechanism for cloud feedback (e.g., Paltridge 1980; Charlock 1982; Somerville and Remer 1984; Somerville and Iacobellis 1987; and Roeckner et al. 1987). The simulations of Roeckner et al. (1987) even suggest that cloud feedback may be positive thus accentuating the warming induced by a CO_2 increase largely due to the increase of cirrus clouds in the simulations.

It is a widespread belief that thin cirrus clouds act to enhance the "greenhouse effect" owing to a particular combination of their optical properties (Manabe and Wetherald 1967; Cox 1971; Stephens and Webster 1981). In the study of Stephens and Webster (1981), and supported by others since (e.g., Ou and Liou 1984), it is argued that the increased emission to the surface by thin cirrus outweighs the solar radiation reduced by reflection from cloud top. This tendency is thought to reverse as the cloud optical thickness increases. It is demonstrated in the present study, however, that this predicted greenhouse effect is perhaps influenced by inadequate treatment of the physics of cirrus clouds in the model and that the more likely impact of cirrus to climate change remains somewhat elusive. These conclusions are developed within the context of a specific feedback mechanism incorporated into a simple "mechanistic" climate model. A specific scientific question addressed here is whether or not the observed relationship between the ice water content and tem-

Corresponding author address: Dr. Graeme L. Stephens, Department of Atmospheric Science, Colorado State University, Fort Collins, CO 80523.

perature of cirrus provides any significant feedback to the CO_2 greenhouse warming. A related question that is also examined concerns the specific role of cloud microphysics and radiation in this feedback. This raises several pertinent issues about our understanding of cirrus clouds and their likely role in climate change as there presently exists a considerable uncertainty about the microphysics of these clouds, such as the size and shape of ice crystals and their radiative influences (e.g., Platt et al. 1989; Prabhakara et al. 1988).

The feedback examined in this paper is defined in the following section and is based on the observed relationship between ice water path and cloud temperature. Section 3 introduces the model that provides the framework for a new parameterization of the albedo and emissivity of clouds. In order to examine the feedback between ice path and temperature it is necessary to establish a connection between cloud albedo, cloud emissivity and ice water path thereby establishing a temperature dependence of these cloud radiative properties. This dependence is formulated in section 4 in which the extinction coefficient (and thus optical depth) and single scattering albedo are obtained as functions of the effective radius of the size distribution and the ice water content. These parameters, together with a specified value of the asymmetry factor and the solar zenith angle provide a complete specification of the cloud radiative properties. Observations are used in section 5 in an effort to estimate values of the effective radius and asymmetry factor typical of cirrus. The parameterizations of cloud albedo and emittance are then incorporated into the climate model described in section 6. A series of climate simulations are described in this section and the ice water feedback mechanism is examined. A summary of the results of the paper and the conclusions drawn from this study are presented in the final section.

2. Cloud microphysics and ice water content

Characterization of the shape and size of ice crystals in terms of their environmental parameters continues to be a subject of extensive research in cloud physics and is a topic that, through the dependence of both cloud albedo and emittance on microphysical parameters, is also crucial to the cloud–climate problem. For environments typical of cirrus clouds, ice crystals exist both in single and polycrystalline forms. The observations of Heymsfield and Platt (1984) indicate that both the size of these ice crystals and the ice water content increases with increasing cloud temperature. Their results are reproduced in Fig. 1 together with an empirical relationship,

$$w(\mathrm{g\ m^{-3}}) = 0.0007e^{0.041(T°\mathrm{C}+60)}, \qquad (1)$$

which is taken to represent these data and provides the basis of the feedback between climate warming and cloud ice mass addressed in this paper as well as in the work of Platt and Harshvardhan (1988). We hereafter refer to this feedback as the ice water content feedback.

3. A model of the albedo and emittance of cirrus

In order to examine the influence of the ice water content feedback on the simple climate simulations reported below, it is first necessary to establish the connection between the cloud radiative properties and the ice water path in the form of a tractable and physically based parameterization. We now outline the cloud radiation model used as the framework for this parameterization. In formulating this model, we are forced to neglect any effects of horizontal cloud structure on radiation since a coherent treatment of this problem is not yet available in radiative transfer theory. In this study, as others have done before (for example, see the review of Stephens 1984), the two-stream model is used as a basis for the parameterization. Description of a variety of two stream models can be found in several review articles on the subject (Meador and Weaver 1980; King and Harshvardhan 1986, among others) so only a very brief outline is presented here.

Derivation of the basic two stream equations and the parameters that define them are described in detail

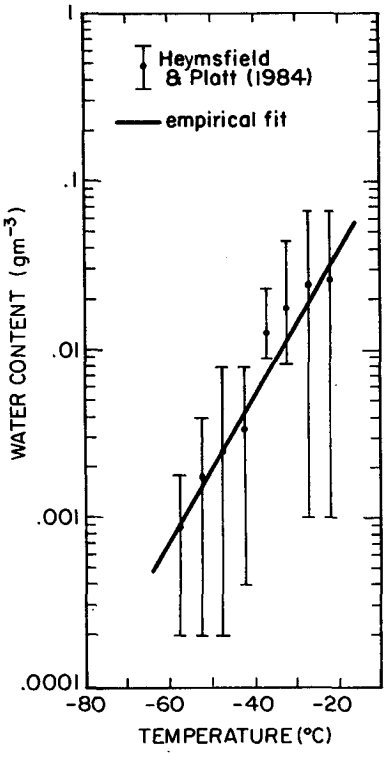

FIG. 1. The relationship between cirrus cloud ice water content and cloud temperature (after Heymsfield and Platt 1984) and the empirical relationship (solid line) expressed by (1).

in the above cited papers. The form of the equations adopted here is

$$\mp \frac{dF^{\pm}}{d\tau} = -[D(1-\tilde{\omega}_o) + \tilde{\omega}_o b]F^{\pm} + \tilde{\omega}_o b F^{\mp} + S^{\pm}_{\text{sol/IR}} \quad (2)$$

where $F^{\pm}$ are the upwelling (+) and downwelling (−) fluxes, D is the diffusivity which is given the value of $\frac{7}{4}$ for solar wavelengths and 1.66 for longwave radiation, and the source terms $S_{\text{sol/IR}}$ refer to the solar (sol) and infrared (IR) sources of flux. The parameters crucial to this equation are

(i) the extinction coefficient α_{ext}: this parameter characterizes the attenuation of radiation along a given path in the cloud. The product of α_{ext} and the vertical path length in the cloud defines the optical depth τ and we hereafter use τ^* to represent the optical depth of the entire cloud layer. In this paper, we provide a parameterization of τ^* in terms of the ice crystal size.

(ii) The single scatter albedo $\tilde{\omega}_o$: this parameter is the ratio of the scattering to total extinction by the cloud particles $\tilde{\omega}_o = \alpha_{\text{sca}}/\alpha_{\text{ext}}$. Thus when $\tilde{\omega}_o = 1$, the cloud is non-absorbing (note the absorption coefficient $\alpha_{\text{abs}} = (1-\tilde{\omega}_o)\alpha_{\text{ext}}$). The single scatter albedo varies strongly with wavelength generally in the range $0.9 < \tilde{\omega}_o < 1$ for shortwave radiation (mainly in the near IR region with $\lambda > 0.7$ μm and is typically less than about 0.6 for longwave radiation. A relationship between $\tilde{\omega}_o$ and particle size is developed in the parameterization described below.

(iii) b, the particle backscatter for diffuse radiation which is related to the asymmetry parameter g. The asymmetry parameter is a measure of the degree of anisotropy of scattering. For completely forward scatter, $g = 1$ while $g = -1$ for total backscatter and $g = 0$ when the scattering is isotropic. For real clouds $g = 0.7$–0.9 and is relatively independent of wavelength. It is shown below that g is an important parameter for the climate simulations described.

a. A model of the cloud albedo

The general solution of (2) is briefly outlined in appendix A and more detail about the solution can be found in the cited references on two stream models. The expression for diffuse reflectance given by (A5), must be modified before it can be used to describe cloud albedo since it excludes any solar zenith angle dependence. This shortcoming is overcome by introducing the contribution to the solar flux at level τ due to the single scatter of a collimated source of flux. The value of this collimated flux perpendicular to the flow at cloud top is taken to be F_o and is transmitted along the direction with a zenith angle cosine of μ_o down to level τ. This flux provides the particular solution of the form (e.g., Preisendorfer 1976, for details)

$$F^{\pm}_{p,\,\text{sol}} = F_0 Z_{\pm}(\mu_o) e^{-\tau/\mu_o}$$

where

$$Z_{\pm}(\mu_o) = \tilde{\omega}_o \left[\frac{\begin{pmatrix} f_o \\ b_o \end{pmatrix} \tilde{\omega}_o b + \begin{pmatrix} b_o \\ f_o \end{pmatrix} \left[D(1-\tilde{\omega}_o) + \tilde{\omega}_o b \mp \frac{1}{\mu_o} \right]}{k^2 - \left(\frac{1}{\mu_o}\right)^2} \right], \quad (3)$$

and where f_o and b_o are the fractions of the collimated sunlight forward and backscattered by the cloud. The albedo of an isolated cloud layer is then obtained from (A1) using

$$F^{-}(\tau = 0) = F_o \quad (4a)$$

for the upper boundary condition and

$$F^{+}(\tau = \tau^*) = 0 \quad (4b)$$

for the condition at cloud base. With these boundary conditions in (A1), it follows that

$$C_- = \frac{F_o}{\Delta(\tau^*_k)} [Z_+(\mu_o) h_- e^{-\tau^*/\mu_o} - Z_-(\mu_o) h_+ e^{\tau^*_k}]$$

$$C_+ = \frac{-F_o}{\Delta(\tau^*_k)} [Z_+(\mu_o) h_+ e^{-\tau^*/\mu_o} - Z_-(\mu_o) h_- e^{-\tau^*_k}] \quad (5)$$

where we introduce the notation

$$\Delta(\tau^*_k) = h_+^2 e^{\tau^*_k} - h_-^2 e^{-\tau^*_k}, \quad (6)$$

and where τ^*_k is the diffuse optical thickness of the cloud layer defined in the appendix A. The albedo, transmittance and absorptance of an isolated cloud layer can be defined as $\mathcal{R} = F^{+}(0)/\mu_o F_o$, $\mathcal{T} = F^{-}(\tau^*)/\mu_o F_o + \exp[-\tau^*/\mu_o]$, and $\mathcal{A} = 1 - \mathcal{R} - \mathcal{T}$, respectively, and from (A5) and (A6) in (A1) we obtain

$$\mathcal{T} = e^{-\tau^*/\mu_o} + \frac{1}{\mu_o \Delta(\tau^*)} \{Z_-(\mu_o)[\Delta(\tau^*) e^{-\tau^*/\mu_o} - \Delta(0)] - Z_+(\mu_o) h_+ h_- e^{-\tau^*/\mu_o}(e^{k\tau^*} - e^{-k\tau^*})\}$$

$$\mathcal{R} = \frac{1}{\mu_o \Delta(\tau^*_k)} \{Z_+(\mu_o)[\Delta(\tau^*_k) - \Delta(0) e^{-\tau^*/\mu_o}] - Z_-(\mu_o) h_+ h_-(e^{\tau^*_k} - e^{-\tau^*_k})\}. \quad (7)$$

These expressions relate the albedo and transmittance of the cloud to the cloud optical thickness, the solar zenith angle and the various scattering parameters that

are imbedded in the definitions of both τ_k^* and $Z_\pm$. The forward and backscatter fractions f_o, b and b_o contained in these definitions are specified according to

$$b = \frac{1}{4}(1 - 1/\tilde{\omega}_o') + \frac{3}{4}(1 - g')$$

$$b_o = \frac{1}{2}(1 - 3_g'\mu_o/D)$$

$$b_o + f_o = 1, \tag{8}$$

given the scaled quantities

$$g' = g/(1 + g)$$

$$\tilde{\omega}_o' = \frac{\omega_o(1 - g^2)}{1 - \omega_o g^2}$$

and using $\tau' = (1 - \omega_o g^2)\tau$ in (7) instead of τ. With these scalings, together with the definitions given by (8), we obtain the δ-Eddington approximation (e.g., Meador and Weavor 1980). In this way, (7) together with (8) defines the cloud albedo and cloud transmittance of a single isolated cloud layer as a function of solar zenith angle μ_o and the optical properties τ, $\tilde{\omega}_o$ and g. The radiation distribution within a multiply layered atmosphere, including the effects of surface reflection, is then modeled using the adding method described previously by Stephens and Webster (1981) given the radiative properties of individual layers.

b. *A generalized model of cloud emittance*

Kirchoff's law is used to describe the source of thermal emission

$$S_{\text{IR}}^{\pm} = (1 - \tilde{\omega}_o)\mathcal{B}(\tau) \tag{9}$$

where $\mathcal{B}(\tau)$ is the Planck blackbody function for flux. For an isothermal cloud layer, the particular solution is

$$F_{p,\text{IR}}^{\pm}(\tau) = \mathcal{B}_o \tag{10}$$

where $\mathcal{B}_o$ is the value of the Planck function determined from the cloud temperature.

We are now in a position to derive the cloud emissivity directly from (A1). The boundary conditions are

$$F^-(0) = F_t \quad \text{cloud top}$$

$$F^+(\tau^*) = F_g \quad \text{cloud base} \tag{11}$$

where F_g is the upwelling flux from the surface below the cloud. For an isothermal cloud (A1) can be written as

$$F^+(0) = \mathcal{T}F_g + \mathcal{B}_o(1 - \mathcal{T} - \mathcal{R}) + \mathcal{R}F_t$$

$$F^-(\tau^*) = \mathcal{R}F_g + \mathcal{B}_o(1 - \mathcal{T} - \mathcal{R}) + \mathcal{T}F_t \tag{12}$$

where $\mathcal{R}$ and $\mathcal{T}$ are the general diffuse reflectance and transmittance defined by (A5)–(A6). As emphasized in other studies (e.g., Stephens 1980), the longwave radiative characteristics of cirrus clouds tend to be dominated by the radiative interactions in the *atmospheric window* spectral region between about 8 and 13 μm. For the sake of illustration, and without any loss of generality (it is straight forward to retain the F_t term), we assume the atmosphere to be transparent in this spectral region such that $F_t = 0$. Using the following definition for emissivity

$$\epsilon = \frac{F^-(\tau^*)}{\mathcal{B}_o}, \tag{13}$$

then from (12)

$$\epsilon = \mathcal{R}F_g/\mathcal{B}_o + \left[1 - \mathcal{R} - \frac{4\gamma e^{-\tau_k}}{(1 + \gamma)^2 - (1 - \gamma)^2 e^{-2\tau_k}}\right]. \tag{14}$$

With the assumption in the infrared that $g \sim 1$ then $\gamma \sim 1$ and $\mathcal{R} \sim 0$, the eigenvalue k in (A2) assumes the property of a diffuse fractional absorption coefficient

$$k = D[(1 - \tilde{\omega}_o)(1 - \tilde{\omega}_o g)]^{1/2} \sim D(1 - \tilde{\omega}_o). \tag{15}$$

With the definition $\tau_{\text{abs}} = (1 - \tilde{\omega}_o)\tau$ for a homogeneous layer, (13) reduces to

$$\epsilon \approx 1 - e^{-D\tau_{\text{abs}}}, \tag{16}$$

which is a form of emissivity that has been extensively used in both the analysis of observational flux data and as a parameterization of cloud IR radiative transfer and is also the parameterization used in this study. The assumption of zero scattering ($g = 1$) trivializes the use of the two stream model as a method of parameterizing the infrared transfer in cirrus clouds. However, the general derivation expressed by (14) provides a framework suitable for future parameterizations that are capable of taking infrared scattering into account. It was noted in an earlier study of Stephens (1980) that the contribution by the $\mathcal{R}$ term in (14) can indeed be significant under certain conditions although it is not considered further here.

4. A parameterization of the cloud optical properties

a. *Shortwave optical properties*

Before the ice water feedback can be dealt with in a climate model, the dependence of cloud albedo (and cloud emittance) on w needs to be established. The basis for the parameterization adopted in this study is described in the work of Ackerman and Stephens (1987). The approach uses the anomalous diffraction theory of van de Hulst (1957) to specify the scattering the extinction efficiencies as a function of wavelength, refractive index and cross sectional area A of the particle size distribution. The utility of the approach was demonstrated by Ackerman and Stephens (1987) for water

droplet clouds and is examined here for ice clouds. The working assumption of the approach requires the particle to be large compared to the wavelength of the radiation so the scheme described here applies more readily to solar radiation.

In order to parameterize A, we introduce the modified gamma function

$$n(r) = \frac{N_o}{\Gamma(p) r_m} \left(\frac{r}{r_m}\right)^{p-1} \exp\left(-\frac{r}{r_m}\right) \quad (17)$$

to characterize the size distribution. It should be emphasized here that r and r_m refer to the radii of spheres of that are equivalent in volume to a nonspherical ice crystal. As such, r_m does not directly relate to a measurable crystal dimension (such as the maximum crystal dimension). In what follows, we vary r_m to study its influence on both cirrus radiative properties and on cirrus cloud–climate feedback. Although a variety of distributions have been used in the literature to describe particle size spectra of clouds, only a few types of functions actually fit observations well. In fact, by suitable choice of parameters, the modified gamma function used in this study defines as a special case the gamma, truncated gamma, exponential, Marshall-Palmer, Khrgian-Mazin among other distributions that have been used to approximate measured size distributions (Flatau et al. 1989). By using this function we are therefore able to treat a variety of size distributions in a simple and consistent way.

In (17), N_o is the total (volume) concentration of crystals, r_m is a characteristic radius of the distribution and p defines the dispersion of the distribution. The characteristic radius r_m and parameter p together define the mode, mean and effective radii according to

$$\begin{aligned} r_{\text{mode}} &= (p-1) r_m \\ r_{\text{mean}} &= p r_m \\ r_e &= (p+2) r_m. \end{aligned} \quad (18)$$

The ice water content w associated with the distribution also follows as

$$w = \frac{4}{3} \pi \rho_{\text{ice}} \int_0^\infty n(r) r^3 dr = \frac{4}{3} \pi \rho_{\text{ice}} N_o r_m{}^3 f(3) \quad (19)$$

where ρ_{ice} is the density of ice,

$$f(m) = \frac{\Gamma(p+m)}{\Gamma(p)} \quad (20)$$

and the cross-sectional area per unit volume of the distribution is

$$A = \pi \int_0^\infty n(r) r^2 dr = \pi N_o r_m{}^2 f(2) = \frac{3}{4} \frac{w}{\rho_{\text{ice}}} \frac{f(2)}{r_m f(3)}. \quad (21)$$

In principle, the density of ice varies according to ice crystal size in a manner described, for example, by Heymsfield (1972). This dependence in principle, complicates (19) and (21). In this study, we assume a fixed value of 0.78 g cm^{-3} for the density of ice and ignore its variation on particle size. The value assumed is somewhat typical of cirrostratus clouds (Heymsfield 1972).

When (19) is substituted into the expression for the extinction efficiency provided by anomalous diffraction theory, we obtain by integration (refer to appendix B for details)

$$\alpha_{\text{ext}} = 2A + \frac{4A}{f(2)} \text{Re}\left\{\frac{p}{u_m(u_m+1)^{p+1}} + \frac{1}{u_m{}^2(u_m+1)^p} - \frac{1}{u_m{}^2}\right\} \quad (22)$$

where Re is the real part of the factor in parenthesis and u_m and $2x_m(n-1)$, $x_m = 2\pi r_m/\lambda$, and n is the complex index of refraction. Note that the correct asymptotic limit $\alpha_{\text{ext}} \to 2A$ is obtained as $x_m \to \infty$. A similar procedure for absorption provides

$$\alpha_{\text{abs}} = A + \frac{2A}{f(2)} \left[\frac{p}{v_m(v_m+1)^{p+1}} + \frac{1}{v_m{}^2(v_m+1)^p} - \frac{1}{v_m{}^2}\right], \quad (23)$$

where $v_m = 4x_m n''$ and n'' is the complex part of the refractive index and the correct blackbody limit is approached as $v_m \to \infty$. The relationship for single scatter albedo then follows from (22) and (23) as

$$\tilde{\omega}_o = \frac{1}{2} - \frac{1}{(p+1)p} \left[\frac{p}{v_m(v_m+1)^{p+1}} + \frac{1}{v_m{}^2(v_m+1)^p} - \frac{1}{v_m{}^2}\right]. \quad (24)$$

Therefore (22) and (24), together with (7) and (8), form the complete set of equations that are needed to calculate the shortwave properties of clouds. Given a value of p, μ_o and g, then α_{ext} and $\tilde{\omega}_o$ can be either expressed directly as a function of r_m and A or as function of r_e and w using (18) to (21).

In this study, we divide the entire solar spectrum into five spectral bands and sum over these bands using a weighting function based on the solar flux data of Thekaekara and Drummond (1971). The central wavelengths of these bands and the weights used to obtain broadband quantities are listed in Table 1. For simplicity, water vapor absorption in the cloud is not taken into account. This omission is not considered important in the present context as the typical values of water vapor absorption in a clear sky saturated layer in the upper troposphere is about one to two percent of the total flux incident on the cloud. Furthermore, the total (water vapor plus ice) shortwave absorption

TABLE 1. The refractive indices ($n = n' - in''$) and solar flux weighting functions for the six bands used to determine the broad band cloud albedo and absorption.

λ (μm)	$n = (n', n'')$	Weight
$\lambda < 0.7$	(1.31, 0)	0.517
0.77	$1.31, .199 \times 10^{-7}$	0.0494
1.05	$1.297, .217 \times 10^{-5}$	0.251428
1.29	$1.291, .132 \times 10^{-4}$	0.058766
1.89	$1.275, .309 \times 10^{-3}$	0.083847
2.46	$1.230, .762 \times 10^{-3}$	0.03957

expected of cirrus clouds are calculated to be significantly smaller than the infrared absorption that dominates the climate effects described below.

Figure 2 provides a plot of the broadband albedo supplied by the parameterization scheme as a function of r_e for two values of the ice water path $W (= \int wdz)$ and μ_o. These results are shown as curves on the diagram and are produced using $p = 2$ and $g = 0.85$. Also shown for comparison and indicated by the symbols are the results of calculations performed using a 24 band multistream radiation model of Tsay et al. (1989) which also includes the effects of water vapor absorption by an amount that assumes ice saturation at −50°C. These model results were obtained using values of α_{ext}, $\tilde{\omega}_o$ and g derived directly from Mie theory for a size distribution expressed by (17) with $p = 2$ applied to each of the 24 spectral bands. On the basis of these comparisons, we conclude that the dependence of albedo on r_e, largely through the influence of r_e on τ^*, is well represented by the parameterization scheme described in this paper at least for the values of μ_o and W chosen.

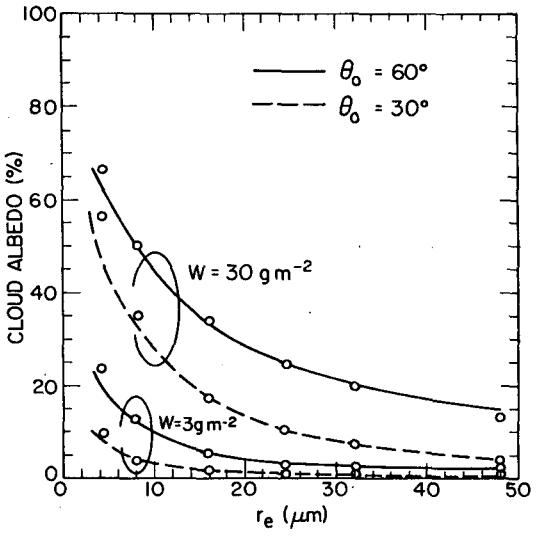

FIG. 2. The parameterized cloud albedo (solid and dashed curves) compared to cloud albedo predicted by a multiband, multistream radiation model using Mie theory. The results are shown as a function of effective radius for two values of solar zenith angle and ice water path.

b. Longwave optical properties

A further simplification of (16) is required to obtain an ice water path dependent cloud emissivity. This modification requires the dubious assumption that the Rayleigh scattering limit for absorbing particles ($4n'\pi r/\lambda < 1$) generally applies for infrared wavelengths. Under this assumption (e.g., van de Hulst 1957), $Q_{abs} \sim cr$, where c is some constant producing the relationship

$$\alpha_{abs} \sim Kw. \tag{25}$$

In this expression the constant K has the gestalt of a mass absorption coefficient. Thus, in the Rayleigh limit, (16) becomes a function of W according to

$$\epsilon = 1 - e^{-DKW} \tag{26}$$

which is the form now commonly used as a parameterization for climate models (e.g., Stephens 1984). Several estimates of K have been derived from both theory and observation for water clouds but relatively few estimates of this parameter exist for ice clouds. A summary of the available observations of cirrus are contained in Table 2. The listed values of Smith et al. (1989) represent the upper and lower range of their values which were derived from flux profiles measured in cirrus and discussed below. They further showed that K varied in an inverse way with the measured maximum crystal dimension.

Under the Rayleigh limit assumption, K is taken to be constant. However, this assumption is questionable for cirrus since K varies in a way which seems to be related to particle size (Smith et al. 1989). We introduce here a size dependent form of K in the following way. The results of several Mie calculations were used to parameterize K in terms of r_e. The Mie calculations were obtained using $\lambda = 11$ μm and the size distribution (17) with $p = 2$, 8, 16 for a fixed value of $w = 0.01$ g m^{-3}. The calculated values of volume absorption coef-

TABLE 2. Comparison of observed and theoretical mass absorption coefficients for cirrus.

K(m^2 g^{-1})	Source, comments ($D = 1.66$)
0.34	Paltridge and Platt 1981: broadband flux emittance
0.051	Paltridge and Platt 1981: effective beam emittance (11 μm)
0.039–0.180	Smith et al. 1988: broadband flux emittance
0.046–0.058	Griffith and Cox 1977: broadband flux emittance in tropical cirrus clouds
0.018–0.068	Platt 1984: derived from the Heymsfield and Platt (1984) data over the temperature range −20° → −60°C.
0.06	Present study; $r_e = 16$ μm, $p = 2$, $\lambda = 11$ μm

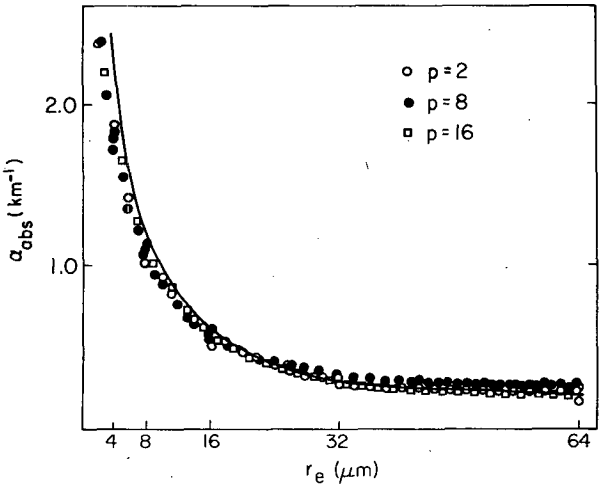

FIG. 3. The relationship between 11 μm volume absorption coefficient and the effective radius as derived from Mie theory using the size distribution given by (17) in the text for the three values of p indicated and for fixed value of $w = 0.01$ g m^{-3}.

ficient are shown in Fig. 3 as a function of r_e as well as the parametric relationship

$$\alpha_{abs}(r_e) = \alpha_{abs}(r_e = 16\ \mu m)16/r_e \qquad (27)$$

(solid curve) for comparison. Since w is fixed in these calculations, the ratio α_{abs}/w, and therefore K, is made to vary inversely with r_e. The physical basis for (27) rests with the assumption that $Q_{abs} \sim$ constant (unity) which is in sharp contrast to (25) and apparently more consistent with the aircraft observations noted. The assumption that $Q_{abs} \approx 1$ at an infrared wavelength of about 10 μm strictly only applies for values of r_e greater than about 15 μm. However, the general inverse relationship employed in this study, according to Fig. 3, seems to be valid over the range of variation of r_e considered in this study. Certainly, a more physically rigorous approach to the parameterization of cloud emissivity as a function of r_e is desirable.

5. An observational study of the relationship between albedo and emittance

As mentioned, the radiative properties of cirrus clouds are parameterized in terms of w, g, p and r_e. In this study, w is derived from (1) given the cloud temperature and both r_e and g are either allowed to vary or specified from the observations in a manner now described. It was shown in the previous study of Ackerman and Stephens (1987) that the albedo is relatively insensitive to p and this parameter is set to the value of 2 in the remaining analyses.

a. Platt's LIRAD observations

The observations reported by Platt and Harshvardhan (1988) are employed here to select the values of r_e that are used in parameterizations described above. Figure 4 shows the values of α_{abs} derived from a series of lidar–radiometer measurements (LIRAD)(e.g., Platt et al. 1987). The additional observations of α_{abs} included on the diagram were obtained from the cited studies which reported on aircraft longwave flux measurements from which ϵ was calculated and α_{abs} in turn derived from (26). Also shown are three relationships calculated from Mie scattering theory for a wavelength of 10.8 μm using (17) with $r_e = 4$, 16 and 64 μm and $p = 2$. The temperature variation of the absorption coefficient arises from the use of (1) in (19) to obtain N_o as a function of temperature. The three theoretical relationships included on the diagram are therefore based on the assumption that r_e is invariant to temperature change and that the increase of ice water content with increasing cloud temperature occurs through an associated increase in total particle concentration. This is, by necessity, an overly simple assumption as already noted and a better understanding of the role that cirrus cloud microphysics play in establishing relationships like that shown in Fig. 4 requires further research. Since we presently lack such an understanding, and at the risk of over simplifications, $r_e = 16$ μm and $p = 2$ seem to represent values of α_{abs} that are typical of the cirrus clouds studied over the temperature range indicated in Fig. 4.

b. Application of aircraft observations to obtain g

Observations of cirrus cloud albedo are generally lacking, and at present it is difficult to verify the predicted dependence of $\mathcal{R}$ on ice water path that is implied in (22) and (24) or that predicted by (26) for ϵ. Hopefully the measurements obtained during the First ISCCP Regional Experiment and the International Cirrus Experiment will provide a dataset capable of testing these schemes. In this section, analyses of aircraft radiometric data are used to obtain $\mathcal{R}$–ϵ relation-

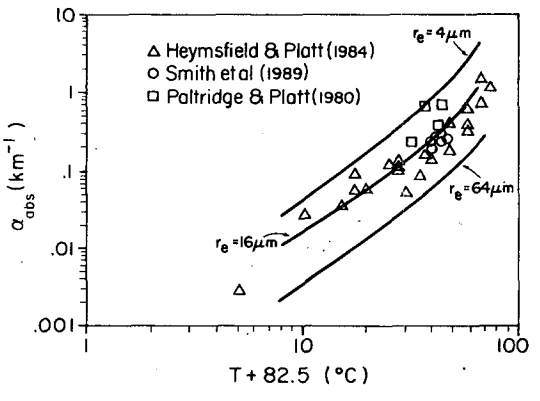

FIG. 4. The observed relationship between volume absorption coefficient and cloud temperature taken from the sources indicated. The three curves were derived from Mie theory for the values of r_e given.

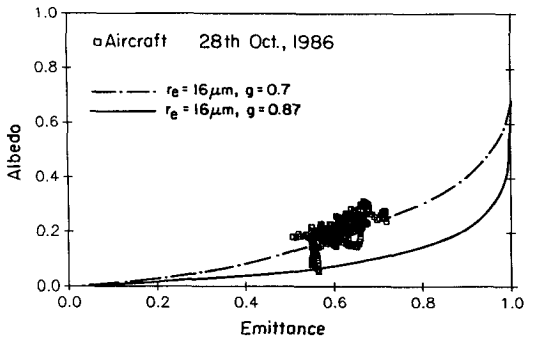

FIG. 5. The relationship between cirrus cloud albedo and emittance derived from aircraft data collected during the 28 October 1986 cirrus FIRE case study. The solid curve is the theoretical relationship derived from Mie theory for spheres with r_e = 16 μm. The dash-dot curve is the relationship derived using a value of asymmetry parameter altered from the Mie value as shown.

ships, which are then matched to theory in such a way that an estimate of the asymmetry parameter is provided.

The aircraft measurements used in this study are those associated with one of the flights conducted in cirrus during the FIRE cirrus field program (Starr 1987). More detailed analyses of the flight data obtained on that day are reported by Smith et al. (1989). The values of $\mathcal{R}$ and ϵ estimated from these broadband flux data are shown in the form of a scatter diagram in Fig. 5. Two theoretical albedo–emittance relationships derived from the parameterization scheme are also shown on Fig. 5. The relationship depicted by the solid curve is that derived assuming ice spheres with r_e = 16 μm and the value of the solar zenith angle corresponding to the time of observation (μ_o = 0.496). The broadband average g determined from Mie theory and used to produce the solid curve is 0.87. The second relationship (dashed curve) provides a better fit to the observations and was obtained with g = 0.7. Other calculations not presented here were carried out using Mie theory with different values of r_e. These calculations resulted in no appreciable change in the relationships given by the solid curve. The need to employ values of the asymmetry factor smaller than those values associated with spherical particles was also pointed out by Platt et al. (1980) in their bispectral analyses of satellite observations.

The difference between the Mie value of g and the value chosen to fit the observations is both significant and expected. It is straight forward to show that the reflectance of thin clouds is directly proportional to the backscatter fraction b_o and hence a function of $1 - g$. The albedo of a cloud estimated using g = 0.7 is therefore greater than the albedo calculated using g = 0.87. We show below that this difference, in turn, significantly influences the predicted response of a climate model to the presence of cirrus cloud. It is also expected that the asymmetry factor of real cirrus clouds composed of irregularly shaped ice crystals is smaller than the asymmetry factor derived for clouds composed of spherical particles (e.g., Stephens 1980).

6. The effects of cirrus optical properties in a simple climate system

We now examine the effects of the cloud optical properties and their relation to ice water content and particle size on a simple climate system. We employ a radiative equilibrium climate model which includes the parameterized effects of convection as used by Stephens and Webster (1981). The intent of this exercise is not to simulate the climate response to variations in cirrus clouds but is directed toward understanding the dependence of surface temperature on the radiative properties of cirrus as well as toward investigating simple aspects of the coupling of the surface temperature to ice water content, cloud microphysics, cloud temperature and radiation.

The climate model employs a convective adjustment scheme similar to that of Manabe and Wetherald (1967). With the exception of the new cloud radiation parameterization described above, the radiative transfer model is that outlined in Stephens and Webster (1981) and is coupled to the convective adjustment scheme to produce a one-dimensional radiative–convective model. Radiative equilibrium is approached iteratively at all levels in the atmosphere except where the resultant temperature gradient between layers exceeds the critical lapse rate value which was set to the moist adiabatic value. The model also invokes the assumption of fixed relative humidity and, together with energy conservation, iterates to a stable radiative–convective temperature profile.

a. Simulations with fixed ice water

The results of a series climate equilibrium experiments using this model are shown in Fig. 6. The results are presented as the difference between overcast and clear sky surface temperature ΔT_g, cloud temperature ΔT_c (upper panel), cloud albedo $\mathcal{R}$ and emittance ϵ (lower panel) as a function of r_e derived at equilibrium. The ice water path prescribed for these experiments is 3 g m^{-2} which corresponds to a 1 km thick cloud at a temperature of 229°K centered about the 37.6 kPa level. The model simulations were carried out using the two values of g employed in the relations shown in Fig. 5 in an effort to demonstrate the sensitivity of the simulated climate to the asymmetry parameter. The resultant surface warming reported in earlier studies like that of Stephens and Webster (1981) is also reproduced in this study. However, the magnitude of this warming is strongly dependent on both the value of g and the value of r_e assumed in the derivation of $\mathcal{R}$ and ϵ. For the simulations with fixed ice path, the surface warming tendency is enhanced by either de-

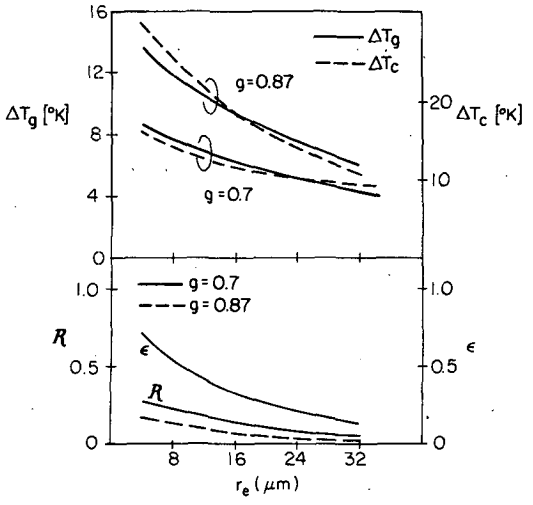

FIG. 6. The difference in the equilibrium surface T_g and cloud T_c temperatures as a function of r_e for two values of asymmetry (upper panel) and the respective change in cloud emittance and albedo as a function of $\mathcal{R}$. The climate simulations were conducted using $\mathcal{R}_g = 0.1$, $F_o = 340$ W m^{-2}, $\mu_o = 0.49$ and a fixed ice water content $W = 3.0$ g m^{-2}. The clear sky equilibrium surface temperature was calculated to be 294.5 K.

creasing the particle size or by assuming more forwardly scattering cloud particles.

A principal driving force of the predicted surface warming is the radiative heating of the cloud layer and the subsequent increased emission to the surface that results primarily from the absorption of upwelling infrared radiation at cloud base. According to the analysis shown in Fig. 6, the cloud warming is more than twice that calculated at the surface. To demonstrate the effect of increasing cloud temperature on surface temperature, the time evolution of the model solutions are displayed on Fig. 7 again in terms of the difference between the overcast and clear sky surface and cloud temperatures. The simulations were carried out with the following prescribed values; $r_e = 16$ μm, $g = 0.7$, and $W = 4.7$ g m^{-2} with the cloud located at the same pressure level as in the previous example. The surface temperature undergoes a slight cooling during the first few simulation days and only significantly differs from the clear sky equilibrium value after about 10 days into the simulation. By contrast, the cloud temperature systematically but unrealistically increases throughout the simulation period. About 10 days into the simulation, the increased emission from cloud base due to the increased cloud temperature is large enough to produce a surface warming which then systematically increases after about 10 days.

b. Simulations with ice water feedback

The ice water feedback was examined by analyzing pairs of control/perturbation simulations with the radiative equilibrium model. The perturbation experiment represents the simulations with twice the present day CO_2 concentration and the control simulations were run with the present day concentrations of CO_2. The notation Δx is used to represent the difference between the perturbation and control simulations of a particular climate parameter of interest (say, surface temperature). Two pairs of perturbation/control experiments are then compared; one pair was conducted with the ice water feedback included in the model and the second pair assumed fixed values of ice water path. These comparisons are presented in terms of the parameter $\delta x = \Delta x$(with feedback) $- \Delta x$(fixed). Positive values of δT_g therefore indicate that the ice water feedback acts to reinforce the simulated CO_2 warming and negative values of δT_g indicate a buffering effect against such a warming.

Values of δT_g, δT_c (upper panel), δW (middle panel) and $\delta\epsilon$ and δR (lower panel) are presented as a function of r_e in Fig. 8. All simulations were performed with $g = 0.7$. These results indicate that the sign of the ice water feedback varies according to the value of r_e used by the model to obtain the cloud optical properties. According to these simulations, the feedback is negative when $r_e < 24$ μm and positive for clouds composed of large crystals. The explanation for this is revealed by comparison of $\delta\mathcal{R}$ and $\delta\epsilon$ and δW. According to the experiments described here, the difference in the cloud emittance between the perturbation and control experiments which include feedback exceeds the respective change in cloud albedo when r_e is large but is less than the change in albedo for smaller values of r_e.

7. Summary and conclusions

This paper examines the effects of cirrus cloud ice water content feedback on climate change. The central question studied in this paper concerns the extent to which both radiative and microphysical properties of cirrus cloud influence this feedback. This question is especially relevant given of the present uncertainty

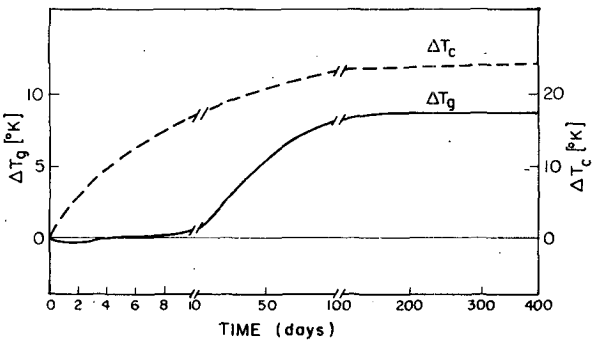

FIG. 7. The time evolution of cloud temperature T_c (dashed) and surface temperature T_g (solid) predicted by the climate model. The results are shown as the difference between the overcast and clear sky equilibrium temperatures and were obtained for the parameters listed in relation to Fig. 6 with $W = 4.7$ g m^{-2} fixed.

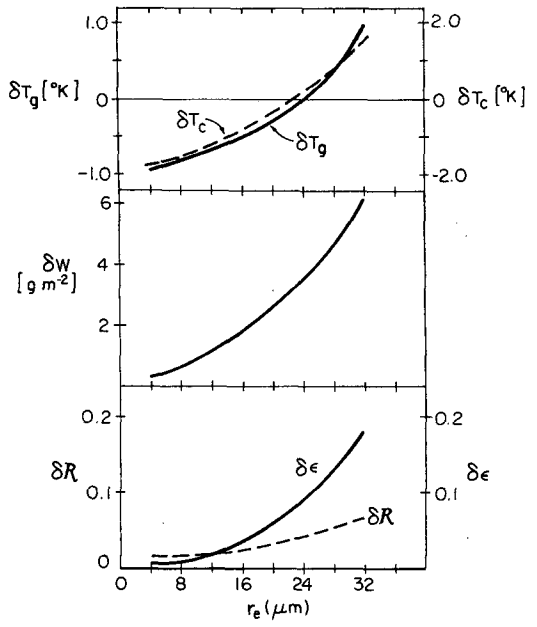

FIG. 8. The feedback analysis parameter δx as defined in the text shown as a function of r_e. Shown are the effects of ice water feedback on the $2 \times CO_2$ simulations of surface temperature, cloud temperature (upper panel), ice water content (middle panel) and cloud albedo and emittance (lower panel). The simulations were carried out assuming the properties listed in relation to the simulations of Fig. 6. Only simulations with $g = 0.7$ are shown.

about the characteristic size of the ice crystals in cirrus clouds.

The major developments of this paper can be summarized as follows:

(i) The importance of the mutual relationship between cloud albedo $\mathcal{R}$ and cloud emissivity ϵ is demonstrated and a new radiation parameterization of these properties is described.

(ii) Observations that relate the ice water content to cloud temperature are incorporated in this parameterization to introduce a temperature dependence to both $\mathcal{R}$ and ϵ. The parameterization of cloud albedo is based on the physical principles of both particle scattering and radiative transfer and is developed in such a way as to emphasize the importance of the cross-sectional area of the particle distribution. This cross-sectional area is further parameterized in terms of the effective radius r_e of the size distribution. In this way, the cloud albedo is therefore expressed as a function of effective radius and asymmetry parameter.

(iii) The parameterization of cloud emittance in terms of the usual bulk absorption arguments is developed directly from radiative transfer theory and the assumptions of the simple emissivity approach are described. A simple parameterization of the particle size dependence of cloud emissivity, previously ignored in other studies of cirrus emittance, is described and is supported by recent aircraft observations.

(iv) The values of the dependent variables, r_e (ratio of the volume to cross sectional area of the size distribution) and g (asymmetry factor), are selected using observations. It is shown that the observed temperature dependence of the infrared volume absorption coefficient noted in the work of Platt and Harshvardan (1988) is reasonably well matched using Mie theory and a single size distribution of spheres with $r_e = 16$ μm. A bispectral analysis of aircraft data provides a $\mathcal{R}-\epsilon$ relationship that on comparison to the parameterization provide an estimate of g. The asymmetry parameter had to be adjusted from the broadband Mie value of $g = 0.87$ for the size distribution chosen to a lower value of $g = 0.7$ in order to bring the observations and theory into broad agreement.

(v) The climate simulations revealed that the predicted effect of cirrus cloud on the surface temperature is sensitive to both r_e and g. Cirrus clouds characterized by $g = 0.87$ warmed approximately twice as much as cirrus clouds modeled with $g = 0.7$. According to the parameterizations used, the surface warming was also predicted to be greater for smaller r_e clouds owing to the more dominant effects of particle size on cloud emittance. The model produces a large increase in the temperature of the cloud layer as a result of the absorption of infrared flux by the cloud. The predicted cloud warming is about twice that calculated for the surface and is the mechanism that drives the surface warming in the model.

(vi) The ice water feedback was examined by analyzing pairs of control/perturbation simulations with the radiative equilibrium model. Comparisons of the $(2 \times CO_2 - 1 \times CO_2)$ simulations with and without cloud feedback revealed that the sign of the ice water temperature feedback on CO_2 warming depends on the value of r_e assumed to represent the radiative properties of the cloud.

The following conclusions are drawn from this paper.

(i) Observations were used in an attempt to define the relationship between cloud albedo and cloud emittance on particle size. While the gross relationships between the relevant cloud optical properties and particle size are poorly understood, a simple idealized model of spherical particles was shown to provide a reasonable match of the observations. Whether this agreement is fortuitous and generally representative of all cirrus is not known.

(ii) The sensitivity of a climate system modeled via assumptions of radiative and convective equilibrium was shown to depend on specific details of ice crystals that are either poorly known (as in the case of r_e) or poorly understood (as for example g). It was also shown that the sign of cloud ice water-temperature feedback varied from positive to negative depending on the specific choice of r_e. Based on these findings, prediction of even the sign of any feedback that might exist between cirrus clouds and climate seems premature.

These predictions are limited by our lack of understanding of the relationship between the size and shape of ice crystals and the gross radiative properties of cirrus and more research should be directed to these issues.

(iii) The feedbacks predicted by the model strongly depend on the radiative budget of the cloud layer itself. The calculated infrared radiation absorbed by the model gave rise to a direct warming of the cloud layer and it was shown that this warming was largely responsible for the associated surface warming. This scenario is clearly unrealistic as dynamic and turbulent motions, induced by the radiative warming, will likely act to alter the structure of real cirrus and perhaps even then alter the character of the feedback studied in this paper. Thus understanding the dynamical aspects of cirrus emerges as an important issue in the study of cirrus cloud feedback to climate.

Acknowledgments. This work was supported by the Atmospheric Sciences Section of the National Science Foundation under Contract ATM-8812353 and Office of Scientific Research of the United States Air Force under Contract AFOSR-88-0143. We also gratefully acknowledge the efforts of S. Lini, who prepared the manuscript.

APPENDIX A

The General Solution for Absorbing Cloud

For an absorbing cloud layer, $\sigma_{abs} > 0$ and $\tilde{\omega}_o < 1$ and the general solution of (2) follows as

$$F^+(\tau) = C_+h_+e^{k\tau} + C_-h_-e^{-k\tau} + F_p^+(\tau)$$
$$F^-(\tau) = C_+h_-e^{k\tau} + C_-h_+e^{-k\tau} + F_p^-(\tau) \quad \text{(A1)}$$

with

$$k = \{(1-\tilde{\omega}_o)D[(1-\tilde{\omega}_o)D + 2\tilde{\omega}_o b]\}^{1/2}, \quad \text{(A2)}$$

$$h_\pm = 1 \pm \gamma, \quad \text{(A3)}$$

and

$$\gamma = (1-\tilde{\omega}_o)D/k \quad \text{(A4)}$$

where $C_\pm$ are constants defined by the boundary conditions. In this expression F_p is the particular solution associated with the sources mentioned above. Before discussing the form of the particular solution, it is useful to consider the solution for a sourceless medium. The albedo of the cloud layer of optical thickness τ^* follows as

$$\mathcal{R} = \frac{F^+(\tau=0)}{F^-(\tau=0)} = (1-\gamma^2)\frac{e^{\tau_k^*} - e^{-\tau_k^*}}{(1+\gamma)^2e^{\tau_k^*} - (1-\gamma)^2e^{-\tau_k^*}} \quad \text{(A5)}$$

and the transmittance as

$$\mathcal{T} = \frac{F^-(\tau=\tau^*)}{F^-(\tau=0)} = \frac{4\gamma}{(1+\gamma)^2e^{\tau_k^*} - (1-\gamma)^2e^{-\tau_k^*}} \quad \text{(A6)}$$

where we introduce

$$\tau_k^* = k\tau^*$$

as the diffuse optical depth.

APPENDIX B

Extinction and Absorption Derived from Anamalous Diffraction Theory

In van de Hulst's anomalous diffraction theory, the particles are assumed to be both large ($x \gg 1$) and soft $|n-1| \ll 1$ where x and n are the size parameter and complex refractive index respectively. The general expression for extinction and absorption by the particle is expressed in terms of the following function (see van de Hulst, ch. 11)

$$\Psi(u) = \frac{1}{2} + \frac{e^{-u}}{u} + \frac{e^{-u}-1}{u^2}. \quad \text{(B1)}$$

where $u = 4\pi r(n-1)/\lambda$ is a complex variable. The extinction efficiency is given as

$$Q_{ext} = 4\,\mathrm{Re}[\Psi(u)], \quad \text{(B2)}$$

and the extinction coefficient follows as

$$\alpha_{ext} = 4\,\mathrm{Re}\left[\int_0^\infty \pi r^2\left(\frac{1}{2} + \frac{e^{-u}}{u} + \frac{e^{-u}-1}{u^2}\right)n(r)dr\right]. \quad \text{(B3)}$$

The following integrals are used to evaluate (B3),

$$I_l = \int_0^\infty r^l n(r)dr = N_o r_m{}^l f(l) \quad \text{(B4)}$$

$$L_l = \int_0^\infty e^{-qr}\, r^l n(r)dr = N_o r_m{}^l f(l)\frac{1}{(qr_m+1)^{p+l}} \quad \text{(B5)}$$

where $q = 4\pi r(n-1)/\lambda$ and all other parameters are defined in relation to (17), (18) and (20). Direct application of these integrals gives (22).

The absorption efficiency predicted by anomalous diffraction theory is written in the form

$$Q_{abs} = 2\Psi(v) \quad \text{(B6)}$$

where v is a real parameter

$$v = 8\pi r n''/\lambda \quad \text{(B7)}$$

and where n'' is the complex part of the index of refraction. The volume absorption coefficient then follows as

$$\alpha_{abs} = 2\int_0^\infty \pi r^2\left(\frac{1}{2} + \frac{e^{-v}}{v} + \frac{e^{-v}-1}{v^2}\right)n(r)dr. \quad \text{(B8)}$$

Again (23) follows using the integral definitions (B4) and (B5).

REFERENCES

Ackerman, S., and G. L. Stephens, 1987: The absorption of solar radiation by cloud droplets: An application of anomalous diffraction theory. *J. Atmos. Sci.*, **44,** 1574–1588.

Charlock, T. P., 1982: Cloud optics as a possible stabilizing factor in climate. *J. Atmos. Sci.*, **38,** 661–663.

Cox, S. K., 1971: Cirrus clouds and climate. *J. Atmos. Sci.*, **28,** 1513–1515.

Flatau, P. J., G. J. Tripoli, J. Verlinde and W. R. Cotton, 1989: The CSU-RAMS cloud microphysics module: General theory and code documentation. Colorado State University, Pap. No. 451, 88 pp.

Griffith, K. T., and S. K. Cox, 1977: Infrared radiative properties of tropical cirrus clouds inferred from broadband measurements. Colorado State University, Pap. No. 269, 102 pp.

Heymsfield, A. J., 1972: Ice crystal terminal velocities. *J. Atmos. Sci.*, **26,** 1348–1351.

——, and C. M. R. Platt, 1984: A parameterization of the particle size spectrum of ice clouds in terms of the ambient temperature and ice water content. *J. Atmos. Sci.*, **41,** 846–855.

King, M. D., and Harshvardhan, 1986: Comparative accuracy of selected multiple scattering approximations. *J. Atmos. Sci.*, **43,** 784–801.

Manabe, S., and R. T. Wetherald, 1967: Thermal equilibrium of the atmosphere with a given distribution of relative humidity. *J. Atmos. Sci.*, **24,** 241–259.

Meador, W. E., and W. R. Weaver, 1980: Two stream approximations to radiative transfer in planetary atmospheres: A unified description of existing methods and a new improvement. *J. Atmos. Sci.*, **37,** 630–643.

Ou, S. C. S., and K-N. Liou, 1984: A two-dimensional radiation turbulence climate model. I: Sensitivity to cirrus radiative properties, *J. Atmos. Sci.*, **41,** 2289–2309.

Paltridge, G. W., 1980: Cloud-radiation feedback to climate. *Quart. J. Roy. Meteor. Soc.*, **106,** 895–899.

——, and C. M. R. Platt, 1981: Aircraft measurements on solar and infrared radiation and the microphysics of cirrus cloud. *Quart. J. Roy. Meteor. Soc.*, **107,** 367–380.

Platt, C. M. R., and Harshvardhan, 1988: Temperature dependence of cirrus extinction: Implications for climate feedback. *J. Geophys. Res.*, **93,** 11 051–11 062.

——, D. R. Reynolds and N. L. Abshire, 1980: Satellite and lidar observations of the albedo, emittance and optical depth of cirrus compared to model calculations. *Mon. Wea. Rev.*, **108,** 195–204.

——, J. S. Scott and A. C. Dilley, 1987: Remote sounding of high clouds. Part VI: Optical properties of midlatitude and tropical cirrus. *J. Atmos. Sci.*, **44,** 729–747.

——, J. D. Spinhirne and W. D. Hart, 1989: Optical and microphysical properties of cold cirrus: Evidence for regions of small ice particles. *J. Geophys. Res.*, **94,** 11 151–11 164.

Prabhakara, C. R. S. Fraser, G. Dalu, Man-Li C. Wu, R. J. Curran and T. Styles, 1988: Thin cirrus clouds: Seasonal distribution over oceans deduced from Nimbus-4 IRIS. *J. Appl. Meteor.*, **27,** 379–399.

Preisendorfer, R. W., 1976: *Hydrological Optics: Vol. V.*, NOAA, ERL,

Roeckner, E., U. Schlese, J. Biercamp and P. Loewe, 1987: Cloud optical depth feedback and climate modeling. *Nature,* **329,** 138–140.

Smith, W. L., Jr., P. F. Hein and S. K. Cox, 1989: The 27–28 October 1986 FIRE IFO cirrus case study: In situ observations of radiation and dynamic properties of a cirrus cloud layer. *Mon. Wea. Rev.*, submitted.

Somerville, R. C. J., and L. A. Remer, 1984: Cloud optical thickness feedbacks in the CO_2 climate problem. *J. Geophys. Res.*, **89,** 9668–9672.

——, and S. Iacobellis, 1987: Cloud-radiation interactions: Effects of cirrus optical thickness feedbacks. *J. Meteor. Soc. Japan,* Special Issue, *Short- and Medium-Range Numerical Weather Prediction.* T. Matsuno, Ed., 177–185.

Starr, D. O'C., 1987: A cirrus-cloud experiment: Intensive field observations planned for FIRE. *Bull. Amer. Meteor. Soc.*, **68,** 119–124.

Stephens, G. L., 1980: Radiative properties of cirrus clouds in the infrared region. *J. Atmos. Sci.*, **37,** 435–446.

——, 1984: The parameterization of radiation for numerical weather prediction and climate models. *Mon. Wea. Rev.*, **112**(Review), 826–867.

——, and P. J. Webster, 1981: Clouds and climate: Sensitivity of simple systems. *J. Atmos. Sci.*, **38,** 235–247.

Thekaekara, M. P., and A. J. Drummond, 1971: Standard values for the solar constant and its spectral components. *Nat. Phys. Sci.*, **229,** 6–9.

Tsay, S-C., K. Stamnes and K. Jayaweera, 1989: Radiative energy budget in the cloudy and hazy Artic. *J. Atmos. Sci.*, **46,** 1002–1018.

van de Hulst, H., 1957: *Light Scattering by Small Particles.* Dover, 470 pp.